ICSV14

Cairns • Australia

9-12 July, 2007

14th International Congress on Sound & Vibration

COMPARISON OF NUMERICAL APPROACHES FOR THE SIMULATION OF SOUND RADIATION FROM A SCARFED INLET

Lukasz Panek, Norbert Schönwald, Frank Thiele

Institute of Fluid Mechanics and Engineering Acoustics
Berlin University of Technology, D-10623 Berlin, Germany

Michael Dumbser, Claus-Dieter Munz

Institut für Aerodynamik und Gasdynamik, Universität Stuttgart, Stuttgart, Germany

lukasz.panek@cfd.tu-berlin.de
norbert.schoenwald@cfd.tu-berlin.de
frank.thiele@cfd.tu-berlin.de
michael.dumbser@iag.uni-stuttgart.de
munz@iag.uni-stuttgart.de

Abstract

In recent decades great effort has been made to reduce the noise emission of aero-engines. Due to increasing bypass ratios the fan area in aero-engines has become larger. This development is advantageous for the efficiency and the reduction of jet noise, however, it relocates the noise problem to the engine intake. In the presented work two different numerical approaches for solving the linearised Euler equations (LEE) will be compared. Their application to the case of sound propagation in the JT15D aero-engine intake will be presented. The fist method, also called the Chimera-technique, is based on overlapping structured grids which exchange data using high order interpolation. It employs the well-known high order Dispersion Relation Preserving scheme (DRP) for the spatial discretisation and an optimised Runge-Kutta Method for temporal integration. The second method is based on unstructured tetrahedral meshes and uses a new version of explicit one-step Discontinuous Galerkin (DG) Finite Element schemes allowing for arbitrary high order of accuracy in space and time as well as for time accurate local time stepping (LTS). Both high order methods are optimised for sound propagation and are capable of simulating complex geometries such as a scarfed nacelle intake including the spinner. The first objective of this work is to gain insight into the acoustic far field characteristics of an intake in the presence of a realistic mean flow. Furthermore, the influence of an asymmetrical shape of the inlet mouth will be studied. The second objective is to compare the different numerical methods with respect to their accuracy and computational efficiency, this being a major criterion for industrial application.

1. INTRODUCTION

It has been shown that high order discretisation is essential for the accurate and efficient simulation of sound propagation problems. Classical structured high order methods are developed for regular grids and may lose their properties when applied to complex geometries. As dictated by blocking constraints, the computational grid in such instance can contain singularities at block joints, point bunchings, kinks or large stretch ratios. In the present paper, two approaches will be presented which alleviate the aforementioned problems. The first, called the Chimera-technique, is an extention of a classical finite differences method to overset grids allowing more freedom in the choice of grid block placement. Besides the usual one-to-one data exchanges on block boundaries, arbitrary exchanges between the host and the overlapping grid are possible. The data transfer is based on high order spatial interpolation to preserve the accuracy of the discretisation scheme. The algorithm was implemented in the TUBA-code of the ISTA.

The second code called Hydsol is based on the recently developed ADER Discontinuous Galerkin (ADER-DG) schemes [1, 2]. This method uses tetrahedral elements for spatial discretisation and is therefore very flexible in terms of handling complex geometries. The order of approximation of the elements can be chosen arbitrarily by the user. It has been very recently extended to allow for *time accurate* local time stepping (LTS) to improve its performance [3]. This becomes important in particular for turbomachinery applications where the mesh generator may produce very small tetrahedral elements at the spinner tip. This would reduce the maximum allowable time step for the entire computational domain if global time stepping algorithms were employed.

To ascertain the assets and drawbacks of the numerical methods, the case of the JT15D aero-engine intake was chosen. It was simulated with both codes while retaining the boundary conditions as well as the mean flow properties. Furthermore, the capabilities of the Chimera method are shown by simulation of a scarfed intake with flight condition using a transformed grid.

2. MATHEMATICAL MODEL

Since the influence of viscosity on sound propagation in air is in most cases negligible, the Euler-Equations can be employed as governing equations. For the simulation, the physical quantities have been split into a time independent steady part representing the mean flow and the unsteady perturbations representing acoustic waves. The linearised form of the Euler-Equations formulated in matrix notation reads as follows

$$\frac{\partial \mathbf{q}}{\partial t} + \mathbf{A} \cdot \frac{\partial \mathbf{q}}{\partial x} + \mathbf{B} \cdot \frac{\partial \mathbf{q}}{\partial y} + \mathbf{C} \cdot \frac{\partial \mathbf{q}}{\partial z} + \mathbf{D}\mathbf{q} = 0 \tag{1}$$

with

$$\mathbf{q} = \left(\varrho', u', v', w', p'\right)^T \tag{2}$$

and

$$\mathbf{A} = \begin{pmatrix} u_0 & \rho_0 & 0 & 0 & 0 \\ 0 & u_0 & 0 & 0 & \frac{1}{\rho_0} \\ 0 & 0 & u_0 & 0 & 0 \\ 0 & 0 & 0 & u_0 & 0 \\ 0 & \gamma p_0 & 0 & 0 & u_0 \end{pmatrix}, \mathbf{B} = \begin{pmatrix} v_0 & 0 & \rho_0 & 0 & 0 \\ 0 & v_0 & 0 & 0 & 0 \\ 0 & 0 & v_0 & 0 & \frac{1}{\rho_0} \\ 0 & 0 & 0 & v_0 & 0 \\ 0 & 0 & \gamma p_0 & 0 & v_0 \end{pmatrix}, \mathbf{C} = \begin{pmatrix} w_0 & 0 & 0 & \rho_0 & 0 \\ 0 & w_0 & 0 & 0 & 0 \\ 0 & 0 & w_0 & 0 & 0 \\ 0 & 0 & 0 & w_0 & \frac{1}{\rho_0} \\ 0 & 0 & 0 & \gamma p_0 & w_0 \end{pmatrix} \tag{3}$$

$$\mathbf{D} = \begin{pmatrix} \frac{\partial u_0}{\partial x} + \frac{\partial v_0}{\partial y} + \frac{\partial w_0}{\partial z} & \frac{\partial \rho_0}{\partial x} & \frac{\partial \rho_0}{\partial y} & \frac{\partial \rho_0}{\partial z} & 0 \\ \frac{1}{\rho_0}\left(u_0 \frac{\partial u_0}{\partial x} + v_0 \frac{\partial u_0}{\partial y} + w_0 \frac{\partial u_0}{\partial z}\right) & \frac{\partial u_0}{\partial x} & \frac{\partial u_0}{\partial y} & \frac{\partial u_0}{\partial z} & 0 \\ \frac{1}{\rho_0}\left(u_0 \frac{\partial v_0}{\partial x} + v_0 \frac{\partial v_0}{\partial y} + w_0 \frac{\partial v_0}{\partial z}\right) & \frac{\partial v_0}{\partial x} & \frac{\partial v_0}{\partial y} & \frac{\partial v_0}{\partial z} & 0 \\ \frac{1}{\rho_0}\left(u_0 \frac{\partial w_0}{\partial x} + v_0 \frac{\partial w_0}{\partial y} + w_0 \frac{\partial w_0}{\partial z}\right) & \frac{\partial w_0}{\partial x} & \frac{\partial w_0}{\partial y} & \frac{\partial w_0}{\partial z} & 0 \\ 0 & \frac{\partial p_0}{\partial x} & \frac{\partial p_0}{\partial y} & \frac{\partial p_0}{\partial z} & \gamma\left(\frac{\partial u_0}{\partial x} + \frac{\partial v_0}{\partial y} + \frac{\partial w_0}{\partial z}\right) \end{pmatrix} \tag{4}$$

The acoustic perturbations were excited using a modal sound source as described by Li et al. [4] located at the fan plane of the duct. The state vector was computed using the following equations

$$\mathbf{q} = A \begin{pmatrix} NJ_m(\mu_{mn}r) + MY_m(\mu_{mn}r) \\ \frac{k}{\omega - M_x k}\left[NJ_m(\mu_{mn}r) + MY_m(\mu_{mn}r)\right] \\ -\frac{i\mu_{mn}}{\omega - M_x k}\left[NJ'_m(\mu_{mn}r) + MY'_m(\mu_{mn}r)\right] \\ \frac{m}{r(\omega - M_x k)}\left[NJ_m(\mu_{mn}r) + MY_m(\mu_{mn}r)\right] \\ \gamma\frac{p_0}{\varrho_0}\left[NJ_m(\mu_{mn}r) + MY_m(\mu_{mn}r)\right] \end{pmatrix} e^{i(\omega t - m\varphi - kx)} \tag{5}$$

$$M/N = -J'(\mu_{mn}R_i)/Y'_m(\mu_{mn}R_i) \tag{6}$$

with J_m and Y_m denoting the m^{th}-order Bessel function of first kind and the Neumann function respectively. The radius R_i corresponds to the spinner radius in the present case. The value of μ_{mn} is chosen to satisfy the hard-wall condition.

3. NUMERICAL METHODS

The Chimera code employs the Dispersion-Relation-Preserving scheme (DRP) proposed by Tam et al. [5] for the spatial discretisation. It has a seven point central stencil with fourth order of accuracy which is optimised to have a wide low-dispersive wave number range. The solution is advanced in time using the LDDRK56 scheme by Hu et al. [6] implemented in the $2N$-storage form proposed by Stanescu et al. [7]. The term "Chimera" refers to the ability of using overlapping grids, which don't necessarily need to have common nodes. To accomplish the communication between the host (underlying) grid and overset grid, high order interpolation is used in both directions. The interpolation coefficients are constant in time and can be computed in advance.

The ADER-DG method of Dumbser et al. implemented in the Hydsol code is discussed in detail in [1, 2]. It is based on discontinuous Galerkin finite elements which are integrated in time not by using a classical Runge-Kutta time stepping method, but using the governing equations themselves via the so-called Cauchy-Kovalewski procedure. This approach leads to a one-step scheme which is uniformly accurate in space and time. The desired order of accuracy can be chosen arbitrarily by the user. To avoid the problem of extremely small time steps dictated by so called sliver elements in automatically generated unstructured tetrahedral meshes, a time accurate local time stepping (LTS) algorithm developed by Dumbser et al. [3] is used. This LTS algorithm, which is obtained in a straightforward manner within the ADER-DG approach, allows for local mesh refinement without throttling the efficiency and is a unique feature among explicit methods.

4. DESCRIPTION OF THE TEST CASE

The JT15D aero-engine geometry was chosen as a test case for the CAA codes. It has been investigated experimentally and proven numerically by many researchers. The computational grids presented here are based on the geometry specified by Baumeister et al. [8], but have been simplified to contain a constant radius inlet lip. The fan plane was extruded to form a buffer zone of constant cross-section to simplify simulation. The exact geometry definition of the simulated case is sketched in Fig. 1. To exploit the Chimera-technique, the geometry described above was

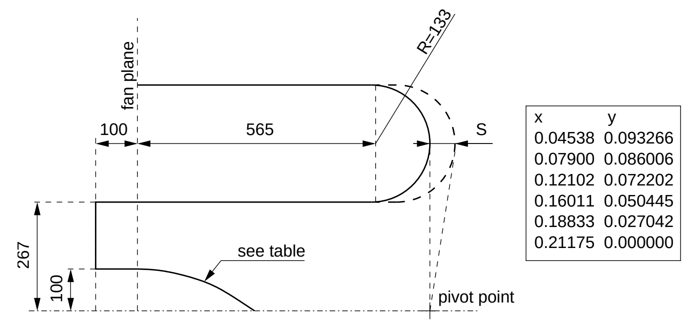

Figure 1. Definition of inlet geometry used for simulations

deformed. The only step to start the simulation of the new geometry is the computation of the new interpolation coefficients. A sine function was used to achieve a scarfing of the inlet lip. The x-coordinate of the overset grid around the lip section was modulated using the following transformation law

$$x_s = x + 0.06\sin(\phi) \tag{7}$$

where x_s is the new position and ϕ the azimuthal angle. The chosen factor of 0.06 results in a scarf angle of approx. 16 degrees. The law retains the lip profile over the circumferential direction, keeping its influence for different azimuthal observer positions constant. A comparison of the original and the scarfed geometry is shown in Fig. 5.

5. RESULTS

The numerical results can be divided into two parts. The first one focuses on the comparison of the numerical methods and is based on the static experiment described by Baumeister et al. [8]. It has a moderate Mach number flow at the fan plane with quiescent ambient air. The Mach number distribution is shown in Fig. 2 (left) as a slice in the xz-plane.

The second part deals with the sound propagation into the far field in the presence of mean flow and in quiescent conditions. For this part only the TUBA-code was employed. Two geometries shown in Fig. 5 were investigated, a symmetrical nacelle and its scarfed variant. The mean velocities were chosen to reproduce a take-off flight condition with a fan plane Mach number of 0.4 and a flight speed of Mach 0.25 at a $3.5°$ angle of attack. The flow fields for both cases are depicted in Fig. 2. All simulations were carried out with modal excitation as described in equation (5) using the (13,0)-mode at 3150 Hz. The far field characteristics were predicted using the acoustic analogy of Ffowcs Williams & Hawkings.

5.1. Comparison of numerical methods

To allow for a reasonable comparison, the size of the computational domain was equal for both the TUBA-code and the Hydsol-code. The grids used for the simulation are shown in Fig. 3. The colored blocks in the semi-structured mesh indicate the overset blocks which communicate

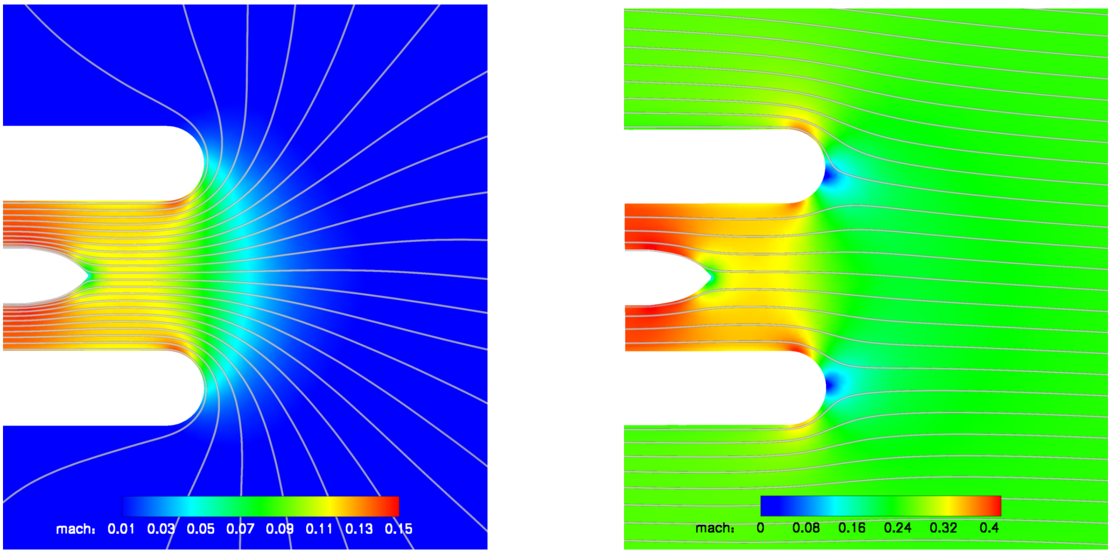

Figure 2. Mach contours and streamlines of the mean flow used as background

with the underlying host grid via interpolation. In radial and axial direction every third point is shown. The unstructured mesh consists of tetrahedral elements and is locally refined near strongly curved boundaries. To compare the solution of both codes, multiple monitor points were defined. Snapshots of the fully developed perturbed pressure fields are shown in Fig. 4.

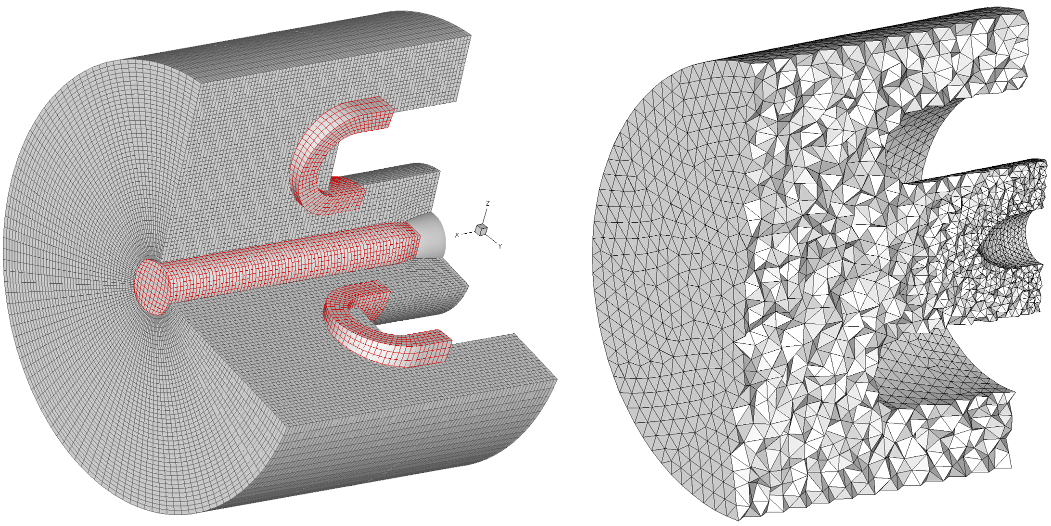

Figure 3. Structured Chimera-grid (left) and unstructured grid (right)

From visual inspection of the plots, both solutions seem to reproduce the principle lobe of the radiation equally well. The analysis of the monitored pressure signals shows a maximum difference of 2 dB in regions of significant sound pressure levels. The computational time needed to simulate one millisecond of physical time for the chosen test case is listed in Table 1 for both codes. The CPUh/ms-value was recalculated for a single CPU or CPU core in case of the dual core Opteron processor. At this point it should be stated that the grids used in the test were not matched to optimally exploit the grid resolution.

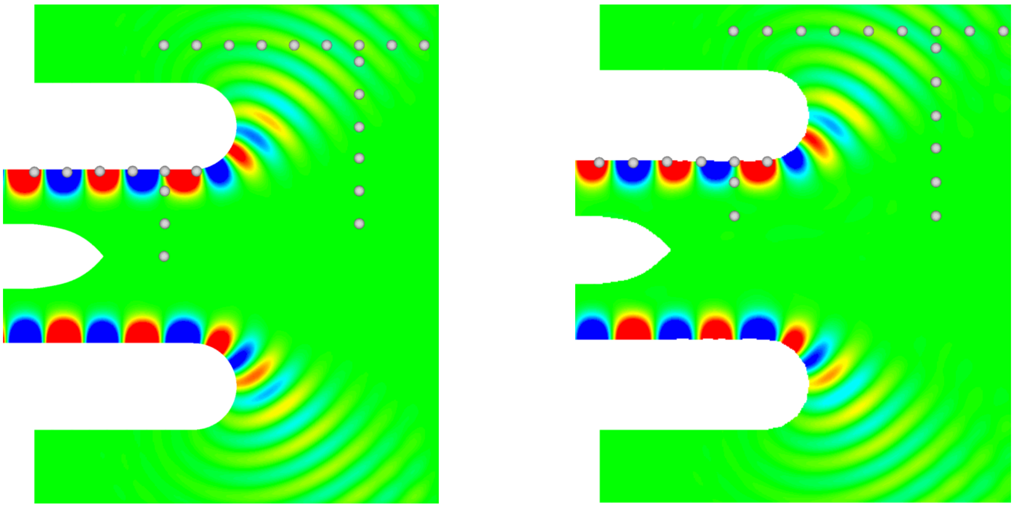

Figure 4. Snapshots of the pressure field computed with the TUBA-Code (Chimera) on the left and the reconstructed field from Hydsol (ADER-DG) on the right, monitoring points are indicated by dots

Table 1. Computational time for the codes under comparison

Code	CPUh / ms	CPU	DOF	Nodes/Elems	Order
TUBA	6.3	Opteron 2.0 GHz, 1 core	5 469 928	5 469 928 N	4^{th}-order
Hydsol	2.15	Xeon 3.6 GHz	2 466 080	123 304 E	P3 Approx.

5.2. Radiation pattern

Figure 5 shows the instantaneous pressure fields simulated with the TUBA-code for two different geometries and two flow conditions. Pictures in the left column (a,b) correspond to the symmetrical nacelle. It's scarfed version is shown on the right side (c,d). The plots for the zero mean flow condition and the flight condition are located in the upper and lower row of the Figure respectively.

During the simulation, the pressure and velocity data on a predefined surface was stored and analysed using the Ffowcs Williams & Hawkings acoustic analogy for observer points located at a radius of 5.42 m around the inlet mouth. The resulting normalised directivity patterns including the static test case with the corresponding experimental data are depicted in Fig. 6. The numerical results of the static test case agree reasonably well with the experiment. I can be observed, that the radiation pattern is very sensitive to the flow properties in the vicinity of the inlet lip.

6. CONCLUSION

Both methods have proven to be capable of simulating the sound propagation in complex geometries accurately. The efficiency of the codes is comparable.

The main advantage of the unstructured method is the simplicity of grid generation. The demand for high quality grids with regard to element size uniformity has been greatly reduced by introducing the local time stepping algorithm. The simple mesh generation also allows to optimize the grid for case parameters such as frequency for each run, thus saving further com-

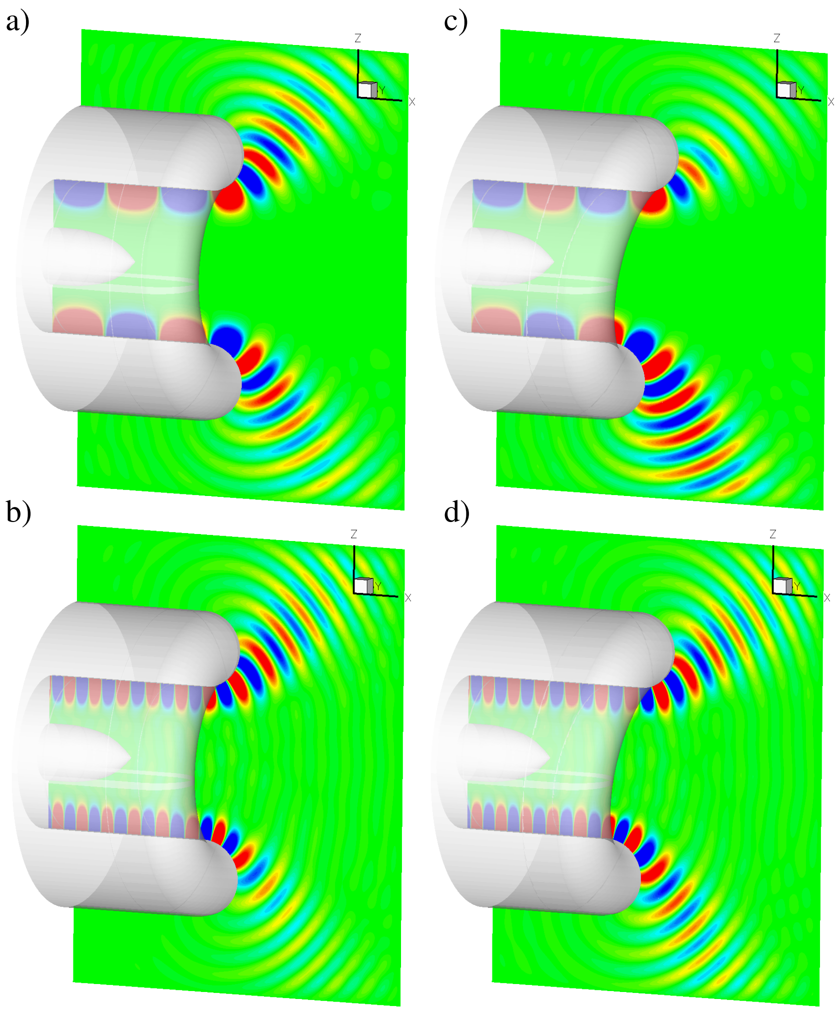

Figure 5. Visualisation of sound propagation for different geometries and flow regimes: a) symmetrical, no mean flow, b) symmetrical, flight conditions, c) scarfed, no mean flow, d) scarfed, flight conditions

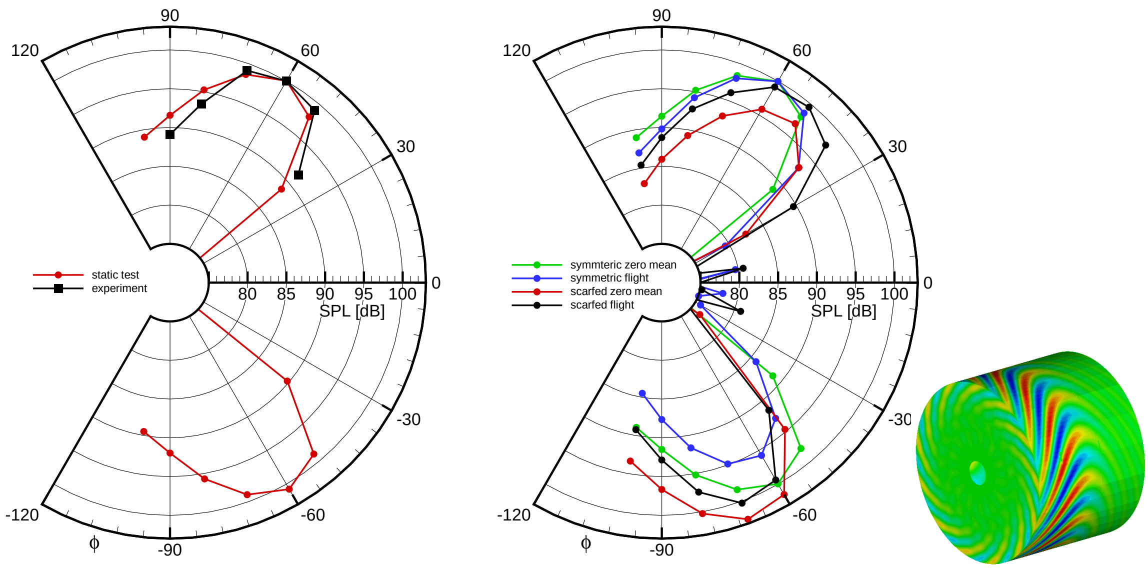

Figure 6. Radiation patterns obtained by means of the Ffowcs Williams & Hawkings acoustic analogy including the integration surface shown right

putational time. Another advantage is the fully automated grid partitioning that is done using the standard METIS software package described in [9].

The Chimera-technique allows to increase the mesh quality by avoiding typical problems caused by blocking constraints. Another advantage of the Chimera-technique is the possibility of changing the case geometry without the need to remesh the physical domain. This feature is useful for optimisation processes.

The analysis of the radiated sound field from an intake showed that the influence of an asymmetrical mean flow can have great impact on the radiation pattern and cannot be neglected in CAA simulations.

REFERENCES

[1] M. Dumbser and C.-D. Munz, "ADER Discontinuous Galerkin Schemes for Aeroacoustics", *Comptes Rendus Mécanique*, Vol **333**, pp. 683–687, 2005

[2] M. Dumbser and M. Käser, "An Arbitrary High Order Discontinuous Galerkin Method for Elastic Waves on Unstructured Meshes II: The Three-Dimensional Isotropic Case", *Geophysical Journal International*, Vol **167**, pp. 319–336, 2006

[3] M. Dumbser, M. Käser and E. F. Toro, "An Arbitrary High Order Discontinuous Galerkin Method for Elastic Waves on Unstructured Meshes V: Local Time Stepping and p-Adaptivity", *Geophysical Journal International, in press.*

[4] X.D. Li, C. Schemel, U. Michel and F. Thiele, "Azimuthal Sound Mode Propagation in Axisymmetric Ducts", *AIAA Journal*, Vol **42**, No. 10, October 2004, pp. 2019–2027

[5] C.K.W. Tam J.C. Webb, "Dispersion-Relation-Preserving Finite Difference Schemes for Computational Acoustics", *Journal of Computational Physics*, Vol **107**, 1993

[6] F.Q. Hu, M.Y. Hussani and J.L. Manthey, "Low-Dissipation and -Dispersion Runge-Kutta Schemes for Computational Acoustics", *Journal of Computational Physics*, Vol **124**, 1996

[7] D. Stanescu and W.G. Habashi, "2N-Storage Low Dissipation and Dispersion Runge-Kutta Schemes for Computational Acoustics", *Journal of Computational Physics*, Vol **143**, 1998, pp. 674–681

[8] K. J. Baumeister and S.J. Horowitz, "Finite Element-Integral Acoustic Simulation of JT15D Turbofan Engine", *ASME Journal of Vibration, Acoustic, Stress, and Reliability in Design*, Vol **106**, July 1984, pp. 405–413

[9] G. Karypis and V. Kumar, "Multilevel k-way partitioning scheme for irregular graphs", *J. Parallel Distrib. Comput.*, Vol **48**, pp. 96-129, 1998.